HEP'99 # 7_230
Submitted to Pa 7
Pl 7, 8

DELPHI 99-78 CONF 265
15 June 1999

Searches for Sleptons using the DELPHI detector at LEP

Preliminary

DELPHI Collaboration

Paper submitted to the HEP'99 Conference
Tampere, Finland, July 15-21

Searches for Sleptons using the DELPHI detector at LEP

Preliminary

P. Allport, A. Galloni, G. J. Hughes, B. King
University of Liverpool
M. Berggren, R. Pain, Ph. Schwemling
LPNHE, University of Paris VI & VII, Paris
S. Martí i García
CERN/EP
S. Amato, M. Gandelman, J.H. Lopes
IF-UFRJ, Rio de Janeiro, Brasil
P. Tortosa
IFIC, Valencia
N. Ghodbane
Institut de Physique Nucléaire de Lyon

Abstract

Data taken by the DELPHI experiment at a center-of-mass energy of 189 GeV and an integrated luminosity of 158 pb^{-1} have been used to search for the supersymmetric partners of the electrons, muons, and taus in the context of the MSSM. Assuming the conservation of R-Parity, Sleptons can be pair-produced. The decay toplogies searched for were the direct decay ($\tilde{\ell} \to \ell\tilde{\chi}_1^0$), producing acoplanar lepton pairs plus missing energy, and the cascade decay ($\tilde{\ell} \to \ell\tilde{\chi}_2^0 \to \ell\gamma\tilde{\chi}_1^0$), producing acoplanar lepton and photon pairs plus missing energy. The observed number of events is in agreement with Standard Model predictions. The 95% CL excluded mass limits have been obtained combining with data taken at lower center-of-mass energies.

1 Introduction

During the 1998 data taking period the LEP accelerator was operating for the first time at centre-of-mass energies of 189 GeV. This increase in energy allowed extension of the searches for scalar partners of electrons (*selectrons*), muons (*smuons*), and taus (*staus*), which are predicted by supersymmetric models. Limits on the production of these particles have already been published based on data taken at centre-of-mass energies of 130-172 GeV, and 183 GeV [1]. This paper reports on a search for these particles in data taken by DELPHI at a centre-of-mass energy of 189 GeV, and shows combined results for this data and the lower energy data.

For these searches the Minimal Supersymmetric Standard Model (MSSM) [2] is assumed, as well as conservation of R-Parity. In this scenario, sleptons could be pair produced via e^+e^- annihilation into Z^0/γ. In addition, selectron production can be enhanced by a contribution from t-channel neutralino exchange, which introduces a direct dependence on the SUSY parameters and the possibility of $\tilde{e}_L$,$\tilde{e}_R$ final states even without mixing via the mass matrix (Figure 1).

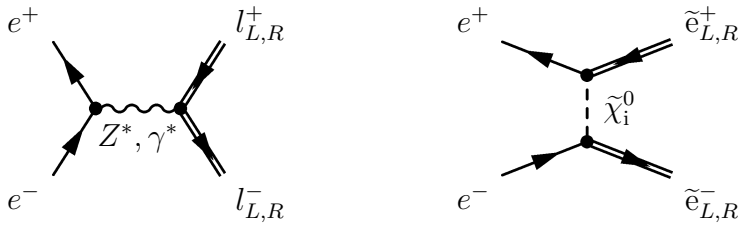

Figure 1: Production diagrams for Sleptons in the MSSM

In a large fraction of parameter space, the dominant decay of the sleptons is to the corresponding lepton flavour plus the lightest neutralino, $\tilde{\ell} \to \ell\tilde{\chi}^0_1$ (Figure 2). The lightest neutralino ($\tilde{\chi}^0_1$) only weakly interacts with normal matter such that the topology described will be characterised by acoplanar lepton pairs together with missing energy. In the first analysis described in this paper, we search specifically for this signature. The results of this search can be interpreted as exclusion regions in the $M_{\tilde{\ell}}, M_{\tilde{\chi}^0_1}$ plane, as presented in Section 6. The searches are described in more detail in Sections 3, and 4.

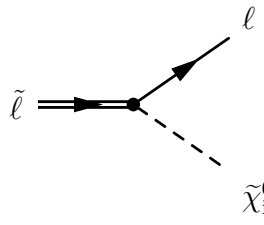

Figure 2: Slepton decay diagram

For certain values of SUSY parameters, it is possible for the second lightest neutralino $\tilde{\chi}_2^0$ to be lighter than the produced sleptons. If this is the case, the slepton can also decay via a cascade to a $\tilde{\chi}_1^0$, with the decay chain $\tilde{\ell} \to \ell\tilde{\chi}_2^0 \to \ell\gamma\tilde{\chi}_1^0$. In order to investigate this channel we have searched our data for events containing acoplanar lepton and photon pairs plus missing energy. This analysis is described in Section 5.

2 Data samples and event generators

The integrated luminosity accumulated at a centre-of-mass energy of 189 GeV by the DELPHI experiment at LEP during 1998 was 158 pb^{-1}. A description of the parts of the DELPHI detector relevant to present paper can be found in [1], while a complete description of the DELPHI detector and its performance can be found in [3].

Simulated events were generated with several different programs in order to evaluate signal efficiency and background contamination. All the models used JETSET 7.4 [4] for quark fragmentation with parameters tuned to represent DELPHI data [5]. The program SUSYGEN [6] was used to generate slepton events and to calculate cross sections and branching ratios.

The generator EXCALIBUR [7] was used to model all four-fermion events, which includes the coherent interference of all diagrams leading to a given final state. For comparison, PYTHIA [4] was used to generate samples of WW, ZZ, Wνe and Zee events. The processes $e^+e^- \to Z^0/\gamma \to q\overline{q}$, including non-resonant t-channel contributions, were simulated by PYTHIA, whilst the two-fermion backgrounds $e^+e^- \to Z^0/\gamma \to \mu^+\mu^-$ and $\tau^+\tau^-$ events were produced by KORALZ [8].

The generators BABAMC and BHWIDE [9] were used to simulate Bhabha scattering. Two-photon interactions leading to hadronic final states were simulated using TWOGAM [10] and BDKRC [11] for the Quark Parton Model contribution. BDK [11] was used for final states with electrons only.

Generated signal and background events were passed through detailed detector response simulation [12] and processed with the same reconstruction and analysis programs as data. The number of background events simulated was mostly several times larger than the number expected in the data.

3 Search for Selectrons and Smuons ($\tilde{\ell} \to \ell\widetilde{\chi}_1^0$)

3.1 Selection of Selectrons

To search for selectrons, the general topology required was acoplanar electrons and missing energy. Selections were tuned both to simulated background events and signal events to reduce the expected Standard Model (SM) background, whilst keeping a reasonable efficiency for the signal over a wide range of the $M_{\tilde{e}} - M_{\tilde{\chi}_1^0}$ combinations.

The preliminary event selection kept all candidates with exactly two well reconstructed oppositely charged particles with momentum above 1 GeV/c. One of the two charged particles was required to be positively identified as an electron, rejecting events if the other was identified as a muon. After this pre-selection good agreement between the data and simulated events is observed (Figure 3).

To reduce the Standard Model backgrounds further cuts were applied. As two-photon events are predominantly at low angles and with low momentum, it was required that the visible energy be greater than 15 GeV and that the energy measured in the low angle STIC calorimeter be less than 4 GeV. As a further constraint, the invariant mass of the two tracks was required to be greater than 4.5 GeV/c^2 .

To reduce the number of Bhabha events an upper limit on the visible energy of 100 GeV was imposed, whilst also requiring the neutral energy not associated to the charged tracks be less than 30 GeV. It was further required that there be no more than four neutral clusters in total. Events from this process are coplanar with a large opening angle, hence it was required that the acoplanarity and acolinearity be greater than 15°.

Four-fermion events were reduced by the cuts described above, in particular the constraint on the visible energy. Cuts were also imposed on the momenta of the two tracks, requiring both tracks to lie in the range 2 GeV $< P <$ 100 GeV. It was further required that the missing momentum vector pointed to an active region of the detector. Finally a lower cut at 5 GeV/c was made on the transverse momentum of the pair of particles.

The efficiency for the signal detection depends on the mass combination of $\tilde{\mathrm{e}}$ and $\tilde{\chi}_1^0$. The cuts used to remove the Standard Model background resulted in typical efficiencies of 50 %.

After this selection 45 candidates were found, compared to 38.5 predicted from background processes.

3.2 Selection of Smuons

The topology searched for was two acoplanar muons and missing momentum. The selection criteria were based on the need to keep signal sensitivity as high as possible for a wide range of $M_{\tilde{\mu}} - M_{\tilde{\chi}_1^0}$ combinations, whilst at the same time rejecting as much of the expected backgrounds as possible. In order to achieve this a different approach was adopted depending on the ($\tilde{\mu}$, $\tilde{\chi}_1^0$) mass difference. For a mass difference ΔM less than 35 GeV/c^2, where two-photon backgrounds are important, an analysis based on sequential cuts was performed. For regions of ΔM greater than 35 GeV/c^2, W-pair backgrounds with the subsequent decay $\mathrm{W^+W^-} \rightarrow \mu^+\nu\mu^-\bar{\nu}$ dominates after a sequential cuts based selection. In this region a probabilistic analysis based on the likelihood of an event being incompatible with W-pair production is used.

As a pre-selection, to select the di-muon topology, exactly two well reconstructed oppositely charged particles with momenta above 1 GeV/c were required. At least one of the particles was identified as a muon. It was further required that neither track be identified as an electron. Good agreement between the data and simulated background events is observed after this stage of the analysis (Figure 4).

For regions of ΔM less than 35 GeV/c^2, a tighter selection based on sequential cuts was used to remove the Standard Model backgrounds. To remove the two-photon events, the visible energy was required to be greater than 10 GeV. Also, the energy in the STIC was required to be less than 1 GeV. As a further constraint the invariant mass of the lepton pair was required to be greater than 4.5 GeV/c^2.

To remove $e^+e^- \to Z^0/\gamma \to \mu^+\mu^-$ events, an upper limit on the visible energy of 120 GeV was imposed, whilst also requiring the unassociated neutral energy to be less than 10 GeV, with no more than two neutral clusters. This background was further reduced by accepting only events in which the opening angle between the tracks was less than 165° and the acoplanarity was greater than 15°.

To reduce W-pair contamination in this low ΔM region, at a small cost in signal efficiency, we reject events in which the positively charged muon is within 40° of the e^+ direction, or the negatively charged muon is within 40° of the e^- direction. Finally, it was required that the missing momentum vector pointed towards active components of the DELPHI detector.

In the regions of ΔM greater than 35 GeV/c^2, a tighter selection based on likelihood discrimination was employed to remove the dominant W-pair background. A discriminating variable was constructed using the following variables:

→ Polar angle and lepton charge (Q Cos(θ))

→ Neutral energy

→ Opening angle between the leptons

→ Acoplanarity

→ Missing energy

→ Missing transverse momentum

The discriminating function is shown in Figure 5, for data, simulated background and simulated signal.

The efficiency for the signal detection depends on the mass combination of $\tilde{\mu}$ and $\tilde{\chi}_1^0$. The cuts used to remove the Standard Model background resulted in typical efficiencies of 50 % for the sequential cuts analysis and 35 % for the likelihood analysis.

Table 2 summarises the number of accepted events in the data, together with the predicted number of events from background sources. For the sequential analysis after the tight selection, 17 candidates remained, consistent with a background prediction of 17.5 events. For the likelihood analysis, 7 candidates remained compared with a background prediction of 9.2 events.

A complementary analysis using a Neural Network approach was also performed. Preliminary results obtained with this method give conclusions consistent with the analysis outlined above.

4 Search for Staus

To select events with a signature of two acoplanar taus and high missing energy, well reconstructed charged and neutral particles were first collected into clusters of total invariant mass below 5.5 GeV/c^2.

Events with exactly two particle clusters (possibly in company with isolated neutral particles) were considered further if there were no more than 6 charged tracks in the event and these gave a total charge of 0 or ± 1. At least two tracks were required to have momentum above 1 GeV/c with one greater than 4 GeV/c.

To remove the two-photon events, these tracks had to be above 30° to the beam axis and there had to be no calorimetric energy below 30°. Also, the direction of the missing momentum should be well in the barrel region ($37° < \theta(\Sigma\vec{p}) < 143°$).

To reduce the background from radiative return to the Z, none of the clusters were allowed to have a total momentum ($p^{\rm JET}$) above 67 GeV/c, isolated photons had to be below 20 GeV and there should be no signal in any 40°tagger [1][3]. Furthermore, the value of the reduced centre-of-mass energy ($\sqrt{s'}$) should not fall in the interval 90.0 to 94.0 GeV around the Z mass. The acoplanarity was required to be between 10° and 176°. In order to further suppress the background from $\rm e^+e^- \to Z^0/\gamma \to \tau^+\tau^-$ events with τ-decays highly asymmetric in visible momentum, the square of the transverse momentum with respect to the thrust axis (δ) had to be above 0.9 (GeV/c)^2.

In order to suppress the W-pair background, the events were analysed under the assumption that they were indeed W-pair events, and the θ angle of the positive W was reconstructed (θ_{W^+}). As W production at 189 GeV is highly asymmetric, while the signal is isotropic, it was demanded that reconstructed angle was $\theta_{W^+} \leq \min(1.5°, -0.05 p^{\rm JET}_{high}({\rm GeV/c}) + 3.7°)$.

This selection was supplemented by cuts that depended on the region of the ($M_{\tilde\tau}$,$M_{\tilde\chi^0_1}$) plane considered which were tuned to remove the corresponding backgrounds for that region: If $\Delta M = M_{\tilde\tau}$-$M_{\tilde\chi^0_1}$ was less than (greater than) 20 GeV/c^2, it was demanded that $p_T^{\rm miss}$ was greater than 5.4 (8) GeV/c. In the lower ΔM region, it was also demanded that the highest momentum of any identified lepton in the event was less than 20 GeV/c. In the higher ΔM region this cut was relaxed to 22 GeV/c.

Table 3 summarises the number of accepted events in the data for the different selections together with the expected numbers of events from the different background channels. 9 candidates were found, at an expected background of 10.6$\pm$0.8 . The efficiencies have been determined using 5000 events for each point of a $1\,{\rm GeV}/c^2 \times 1\,{\rm GeV}/c^2$ grid in the ($M_{\tilde\tau}$,$M_{\tilde\chi^0_1}$) plane, using a fast detector simulation. The results have been verified with the full detector simulation and analysis chain.

5 Search for $\ell\ell\gamma\gamma$ events

There are regions of the SUSY parameter space were the sleptons may also decay into the $\tilde\chi^0_2$ plus the corresponding lepton flavour. The $\tilde\chi^0_2$ may decay to $\tilde\chi^0_1\gamma$, with the $\tilde\chi^0_1$ being the LSP which escapes undetected. The topology for these events is acoplanar lepton pairs and two photons plus missing energy. The main advantage of searching for this type of event is that the experimental signature is very clean with very small Standard Model backgrounds as the emission of photons requires higher orders and extra α_{EM} factors. However the chain decay requires extra branching ratios that may be small, thus suppressing this decay mode. This is especially true for the $BR(\tilde\chi^0_2 \to \tilde\chi^0_1\gamma)$ which is only close to 1 when both neutralinos have a similar mass, but in that case the outcoming photon has low energy, making detection difficult.

The search for these events is done in a two step procedure. First a sample consisting

mostly of standard $\ell\ell\gamma\gamma$ events is selected following some loose cuts. At this level the main data and simulated background are checked to be in agrement. Before applying a tighter selection a likelihood function is defined for the main channel contributing to the sample. Then the tight selection is combined with the likelihood in order to remove those events compatible with the Standard Model processes.

Two likelihood probabilities were constructed, one for tagging Bhabha events in the $ee\gamma\gamma$ sample and the second one for tagging the $e^+e^- \to \mu^+\mu^-$ entering the $\mu\mu\gamma\gamma$ samples. The variables used in the likelihoods were chosen because of their good data – simulated background agreement, their discrimination power between the signal and the background and their low correlation.

5.1 $ee\gamma\gamma$ selection

A standard sample of $ee\gamma\gamma$ events was selected requiring only charged tracks recontructed with momentum greater than 4 GeV/c and at least two photons reconstructed with energy above 1 GeV. Only the two most energetic photons were retained for the analysis, and both charged particles had to be identified as electrons. An acceptance cut demanding that all particles should be in the $10^\circ < \theta < 170^\circ$ region was applied in order to remove most of the two-photon interactions. The same cut was applied to the missing momentum vector, since this can be close to the beam axis for radiative returns. Finally the acolinearity of the electron and photon pairs had to be larger than 3°. With this selection, 164 events were found in data compared to a background expectation of 185 from SM processes. The agreement between the data and the background simulation is shown in Figure 7.

The Bhabha likelihood was built according to the probability density functions (p.d.f.s) of the visible energy, invariant mass between the electron-photon pair with smallest opening angle, the invariant mass of the electron pair and most energetic photon, and the angle between the missing momentum and the closest electron and photon. Figure 7 shows the data and background simulation comparison of the Bhabha likelihood probability.

A sample with most SM events removed was selected by demanding that the events satisfying the standard $ee\gamma\gamma$ selection comply with the following cuts: acolinearity and acoplanarity of the electron and photon pairs above 6° plus Bhabha probability less than 3%. According to this selection, only 3.0 ± 0.7 events were expected from the SM and 4 seen (Table 4).

The detection efficiency was computed for a range of points of the SUSY parameter space and then extrapolated to where the leptons and photons have the same energy; the energy being a function of the mass differences $\tilde{\mathrm{e}}$ – $\tilde{\chi}_2^0$, $\tilde{\chi}_2^0$ – $\tilde{\chi}_1^0$. Typical efficiencies for detection were of the order of 40%.

5.2 $\mu\mu\gamma\gamma$ selection

The selection of a sample of standard $\mu\mu\gamma\gamma$ events proceeded in a similar manner to that of the $ee\gamma\gamma$ events. It was required that at least one of the charged tracks had to be identified as a muon, and none of them as electron. The rest of the cuts were the same as mentioned above. In addition, of those events having more than two photons, only those in which the total energy of the third and consecutive photons was below 10 GeV were retained.

The number of events entering in the standard $\mu\mu\gamma\gamma$ selection was substantially smaller than in the $ee\gamma\gamma$ mainly due to the difference in cross section for Bhabha and $e^+e^- \to \mu^+\mu^-$ processes. 21 events were expected to enter in this sample from the SM prediction, whilst 23 were actually seen.

The $e^+e^- \to \mu^+\mu^-$ likelihood was built from the p.d.f.s of the visible energy, momentum of the leading muon, invariant mass of the muon pair with the most energetic photon, the angle between the missing momentum and the closest muon, and the opening angle of the muon pair.

The tight $\mu\mu\gamma\gamma$ selection consisted basically of the same topological cuts as the tight $ee\gamma\gamma$ selection. In addition to these cuts, it was required that the likelihood for and event being consistent with $e^+e^- \to \mu^+\mu^-$ be less than 5%. With these cuts 2.1 ± 0.5 events were expected from the SM and only 1 seen in the data (Table 5). Typical efficiencies for detection were of the order of 45%.

6 Results

Limits on sfermion masses can be derived using several different assumptions. Scalar mass unification suggests lower masses and cross sections for the partners of right handed fermions. Hence we have assumed that only right-handed selectrons and smuons are produced, leading to conservative mass limits. For third generation sfermions, Yukawa couplings can be large, leading to an appreciable mixing between the pure weak hypercharge states. The production cross section depends on this mixing, due to the variation in strength of the coupling to the Z component of the weak current, and has a minimum at a mixing angle of 45°. For the staus, we therefore present results for this case also.

For each $\tilde{\ell}$ - $\tilde{\chi}_1^0$ mass combination we compare the predicted number of SUSY events with the observed number of kinematically compatible data and background candidates to give the 95 % CL exclusion region.

We have also produced mass limits treating an independent simulated background sample as if it were data to give the MC expected exclusion region.

6.1 Exclusion limits

Exclusion limits on $\tilde{e}_R\tilde{e}_R$ production were obtained taking into account the signal efficiencies for each $M_{\tilde{e}}$-$M_{\tilde{\chi}_1^0}$ point. The limits were calculated for $\mu = -200$ and $\tan\beta = 1.5$. Figure 9 shows the 95% CL exclusion regions obtained by combining the 189 GeV data with lower energy data [1]. For the selectrons, a mass limit can be set at $\tilde{e}_R \geq 87$ GeV/c^2 for mass differences between the selectron and the LSP above 20 GeV/c^2.

Exclusion limits on $\tilde{\mu}_R\tilde{\mu}_R$ production were obtained taking into account the signal efficiencies for each $M_{\tilde{\mu}}$-$M_{\tilde{\chi}_1^0}$ point. Figure 10 shows the 95% CL exclusion regions obtained by combining the 183 GeV data [1] and the 189 GeV data. For the smuons, a mass limit can be set at $\tilde{\mu}_R \geq 80$ GeV/c^2 for mass differences between the smuon and the LSP above 15 GeV/c^2.

Exclusion limits on $\tilde{\tau}\tilde{\tau}$ production were obtained taking into account the signal efficiencies for each $M_{\tilde{\tau}}$-$M_{\tilde{\chi}_1^0}$ point. When determining whether data or background events were kinematically compatible with the mass-point, the end-point of the expected momentum spectrum of the visible reconstructed τ was used. Figure 11 shows the 95% CL $\tilde{\tau}_R$

exclusion region obtained by combining the previous data at 130, 136, 161, 172, and 183 GeV data with the 189 GeV data, and Figure 12 shows the exclusion regions in the case of the mixing angle yielding the minimal cross-section. In the latter plot, data taken at 189 GeV were used for regions where $M_{\tilde{\tau}} > 25$ GeV/c^2, the lower regions being excluded by previous analyses [1]. Due to the vanishing coupling to the Z at this mixing angle, no limit can be inferred form the precision measurements at LEPI in this case. For the staus, a mass limit can be set at 73 to 75 GeV/c^2 (depending on mixing) for mass-differences between the stau and the LSP above 15 GeV/c^2.

For the cascade decay analysis, assuming $\tilde{e_R}\tilde{e_R}$ or $\tilde{\mu_R}\tilde{\mu_R}$ production, one can set exclusion limits in the SUSY parameter space. To set limits one has to consider the cross section for the selectron and smuon production, the branching ratios squared for the $\tilde{\ell} \to \ell\tilde{\chi}_2^0$ and the branching ratio squared for the $\tilde{\chi}_2^0 \to \tilde{\chi}_1^0\gamma$. These cross sections and branching ratios (Figure 13) depend on the actual values of the SUSY parameters. The excluded regions for a given value of the common scalar mass, M_0, and $\tan\beta$ are presented in Figure 14 as a function of the Higgs superfield mass parameter μ and the SU(2) gaugino mass at the EW scale (M).

7 Conclusions

In a data sample of 158 pb^{-1} collected by the DELPHI detector at a centre-of-mass energy of 189 GeV, searches were performed for events with acoplanar lepton pairs.

For the selectron pairs, forty five candidates remained after selection, consistent with the background expectation. Combining this data with our previous lower energy data, a mass limit for $\tilde{\mathrm{e}}_R$ can be set at 87 GeV/c^2 if the the mass-difference between the selectron and the LSP is above 20 GeV/c^2.

In the search for smuon production seventeen events were selected by a sequential cuts approach, consistent with the number expected from Standard Model processes. A likelihood based analysis, used in regions of large $\tilde{\mu} - \tilde{\chi}_1^0$ mass difference, yielded 7 candidates with a background expectation of 9.2 events. Combining this data with our previous lower energy data, a mass limit for $\tilde{\mu}_R$ of 80 GeV/c^2 was obtained, providing the mass-difference between the smuon and the LSP is above 15 GeV/c^2.

In the search for stau production nine events were selected, consistent with the expectation of the Standard Model. Combining this data with all our previous data at centre-of-mass energies 130, 136, 161, 172, and of 183 GeV, a mass limit for the stau can be set at 75 GeV/c^2 if the stau is purely a partner to the right-handed τ, and at 73 GeV/c^2 in the case the stau mixing angle is such that the production cross-section is minimal. These limits are valid if the mass-difference between the stau and the LSP is above 15 GeV/c^2.

Event with the topology of $\mathrm{e^+e^-}\gamma\gamma$, $\mu\mu\gamma\gamma$, and missing energy were searched for and no excess over Standard Model processes were found. This allowed limits to be placed on several MSSM parameters.

These results extend substantially the slepton mass exclusion limits previously obtained.

Acknowledgements

We express our gratitude to the members of the CERN accelerator divisions and compliment them on the fast and efficient commissioning and operation of the LEP accelerator in this new energy regime.

References

[1] P. Abreu *et al.*, DELPHI Collaboration, "*Search for Sfermions at* $\sqrt{s}$ *= 130 to 183 GeV*", contributed to ICHEP98, Vancouver, July 1998..

[2] P. Fayet and S. Ferrara, Phys. Rep. **32** (1977) 249;
H.P. Nilles, Phys. Rep. **110** (1984) 1;
H.E. Haber and G. L.Kane, Phys. Rep. **117** (1985) 75.

[3] DELPHI Collaboration: P. Abreu *et al.*, Nucl. Instr. and Meth. **A303** (1991) 233;
DELPHI Collaboration: P. Abreu *et al.*, Nucl. Instr. and Meth. **A378** (1996) 57.

[4] T. Sjöstrand, Comp. Phys. Comm. **82** (1994) 74;
T. Sjöstrand, "*High energy physics event generation with* `PYTHIA 5.7` *and* `JETSET 7.4`", CERN TH/7111-93 (1993, rev. 1994).

[5] DELPHI Collaboration: P. Abreu *et al.*, Z. Phys. **C73** (1996) 11.

[6] S.Katsanevas and S.Melachroinos in "*Physics at LEP2*", CERN 96-01, Vol.2, p.328.

[7] F.A. Berends, R. Pittau, R. Kleiss, Comp. Phys. Comm. **85** (1995) 437.

[8] S. Jadach, B. F. L. Ward, and Z. Was, Comp. Phys. Comm **79** (1994), 503-522.

[9] S. Jadach, W. Plazeck and B.F.L Ward, HEP-PH/9608412.

[10] S. Nova, A. Olshevski, and T. Todorov, *A Monte Carlo event generator for two photon physics*, DELPHI note 90-35 PROG 152. Behrends Kleiss, etc...

[11] F. A. Berends, P.H. Daverveldt, R. Kleiss, Monte Carlo Simulation of Two-Photon Processes, Comp. Phys. Comm. **40** (86) 271-284.

[12] `DELSIM` *Reference Manual*, DELPHI note, DELPHI 87-97 PROG-100.

Observed events	45
Total background	38.5 ± 0.3
$Z^0/\gamma \rightarrow (\mu\mu,ee,\tau\tau)(n\gamma)$	1.42 ± 0.1
4-fermion events	34.22 ± 0.3
$\gamma\gamma \rightarrow ee,\mu\mu,\tau\tau$	2.23 ± 0.1

Table 1: Selectron candidates, together with the total number of background events expected and the contributions from major background sources for centre-of-mass energy of 189 GeV.

	Sequential	Likelihood
Observed events	17	7
Total background	17.5 ± 0.3	9.2 ± 0.2
$Z^0/\gamma \rightarrow (\mu\mu,ee,\tau\tau)(n\gamma)$	0.86 ± 0.1	1.6 ± 0.2
4-fermion events	15.71 ± 0.32	5.52 ± 0.12
$\gamma\gamma \rightarrow ee,\mu\mu,\tau\tau$	0.94 ± 0.1	2.1 ± 0.2

Table 2: Smuon candidates, together with the total number of background events expected and the contributions from major background sources for centre-of-mass energy of 189 GeV.

Observed events	9
Total background	10.6 ± 0.8
$Z^0/\gamma \rightarrow (\mu\mu,ee,\tau\tau,q\overline{q})(n\gamma)$	1.51 ± 0.20
4-fermion events	7.22 ± 0.35
$\gamma\gamma \rightarrow \tau^+\tau^-$	0.77 ± 0.34
$\gamma\gamma \rightarrow ee,\mu\mu,\ q\overline{q}$	1.12 ± 0.49

Table 3: Stau candidates, together with the total number of background events expected and the contributions from major background sources for centre-of-mass energy of 189 GeV.

Observed events	4
Total background	3.0 ± 0.7
Bhabha	1.5±0.4
$\gamma\gamma \to \tau^+\tau^-$	1.0±0.5
$e^+e^- \to \tau^+\tau^-$	0.4±0.2
4-fermion	0.1±0.1

Table 4: Break down of the individual contributions to the tight $ee\gamma\gamma$ sample.

Observed events	1
Total background	2.1 ± 0.5
$e^+e^- \to \mu\mu$	0.7±0.3
$e^+e^- \to \tau\tau$	0.8±0.3
4-fermion events	0.6±0.1

Table 5: Break down of the individual contributions to the tight $\mu\mu\gamma\gamma$ sample.

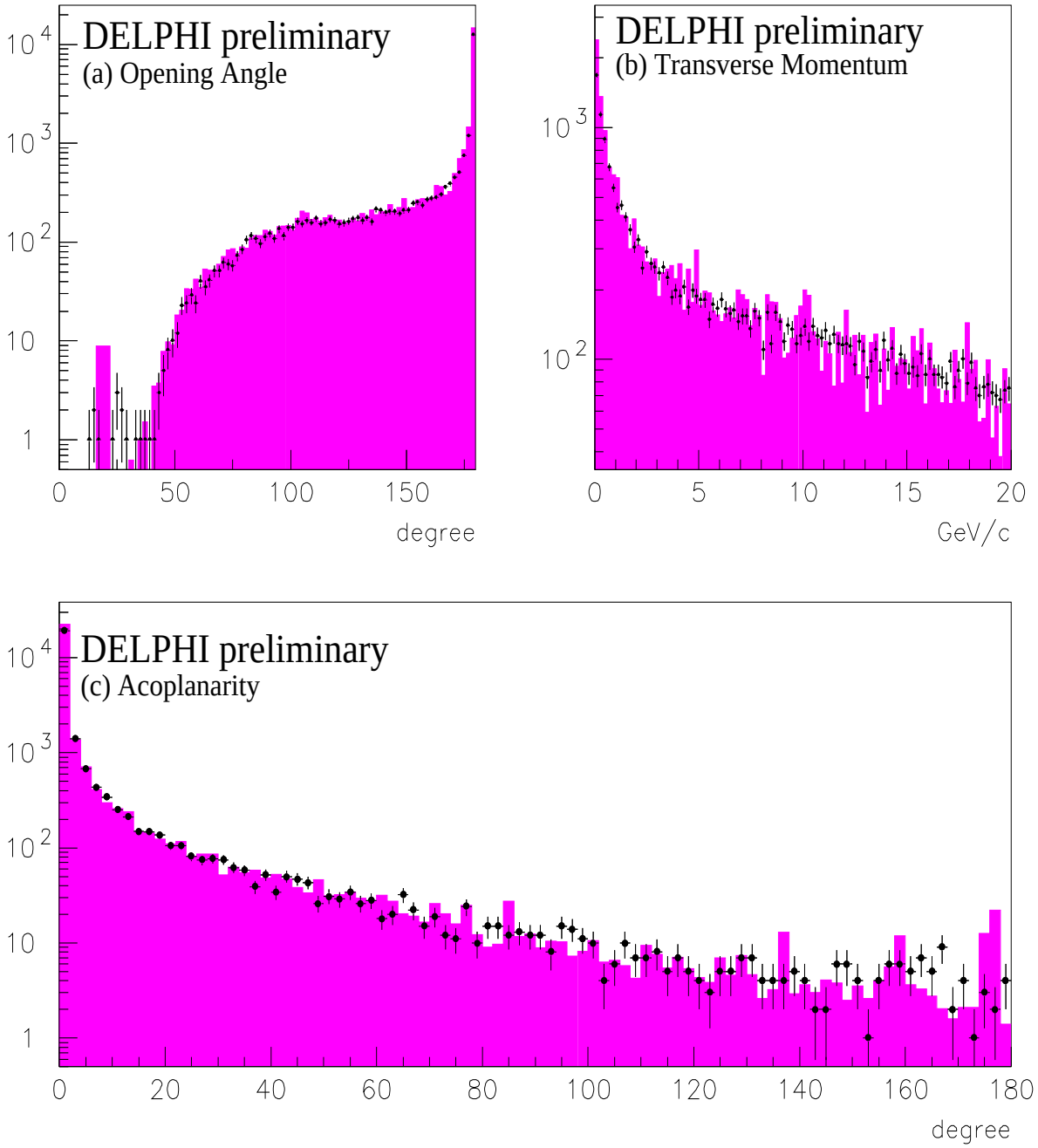

Figure 3: A pre-selection comparison of data and simulation in the selectron analysis. The plots show; (a) Opening angle of the electron pair, (b) Transverse momentum of the electron pair, (c) The acoplanarity. The dots with error bars show the data, while the simulation is shown shaded.

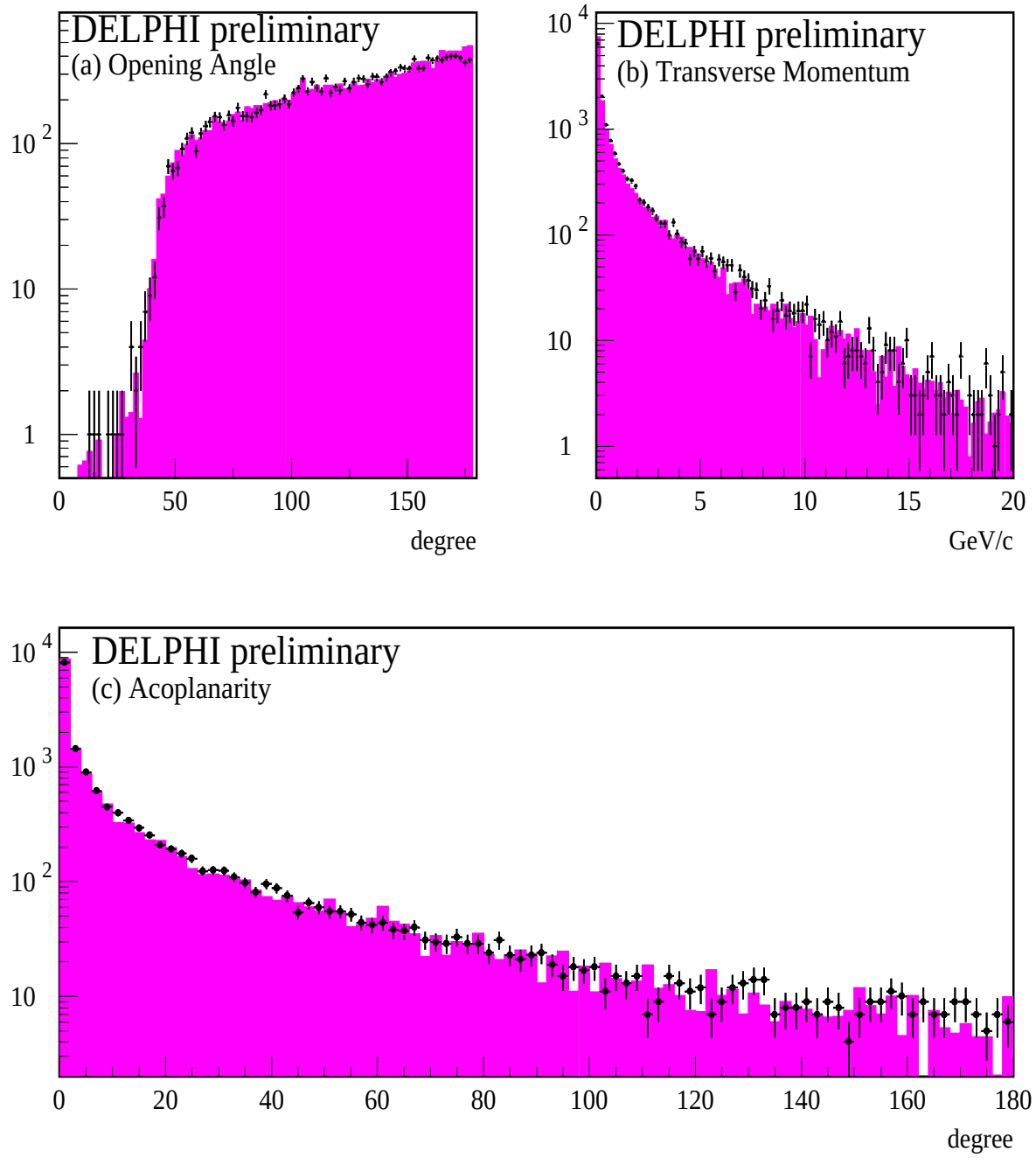

Figure 4: A pre-selection comparison of data and simulation in the smuon analysis. The plots show; (a) Opening angle of the muon pair (b) Transverse momentum of the muon pair, (c) The acoplanarity. The dots with error bars show the data, while the simulation is shown shaded.

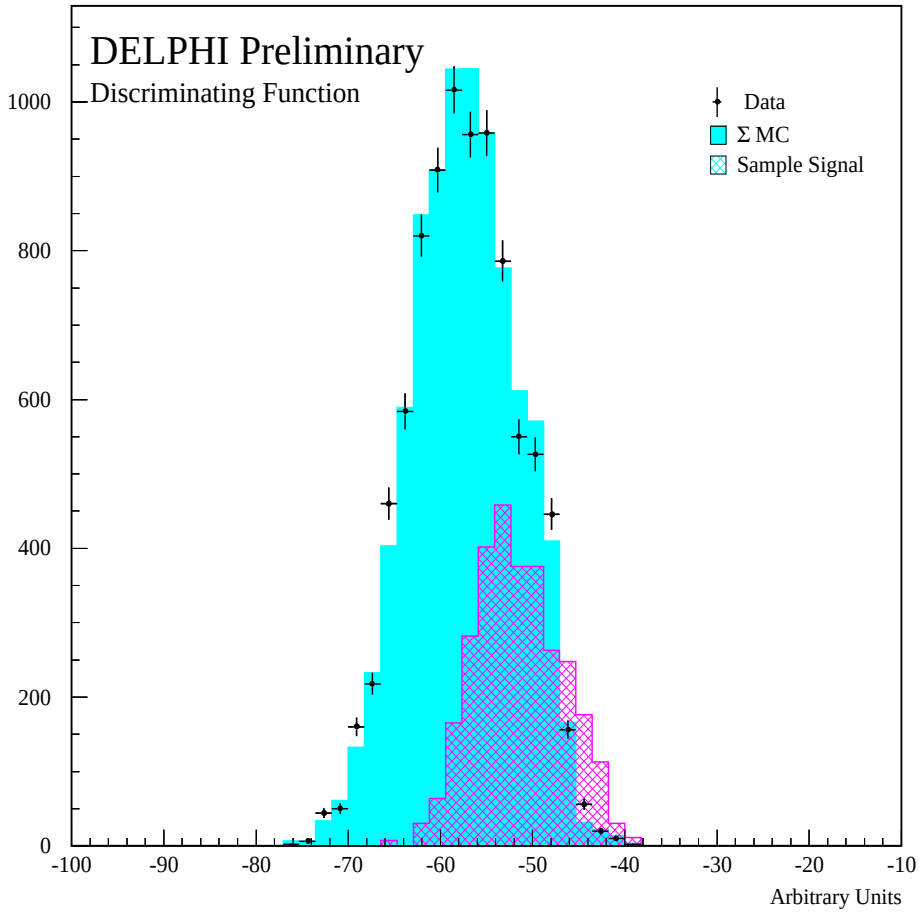

Figure 5: Function produced to discriminate against W-pair backgrounds. The points represent the data and the solid histogram shows the contribution from Standard Model backgrounds. Shown also in the hashed histogram is the expected signal distribution.

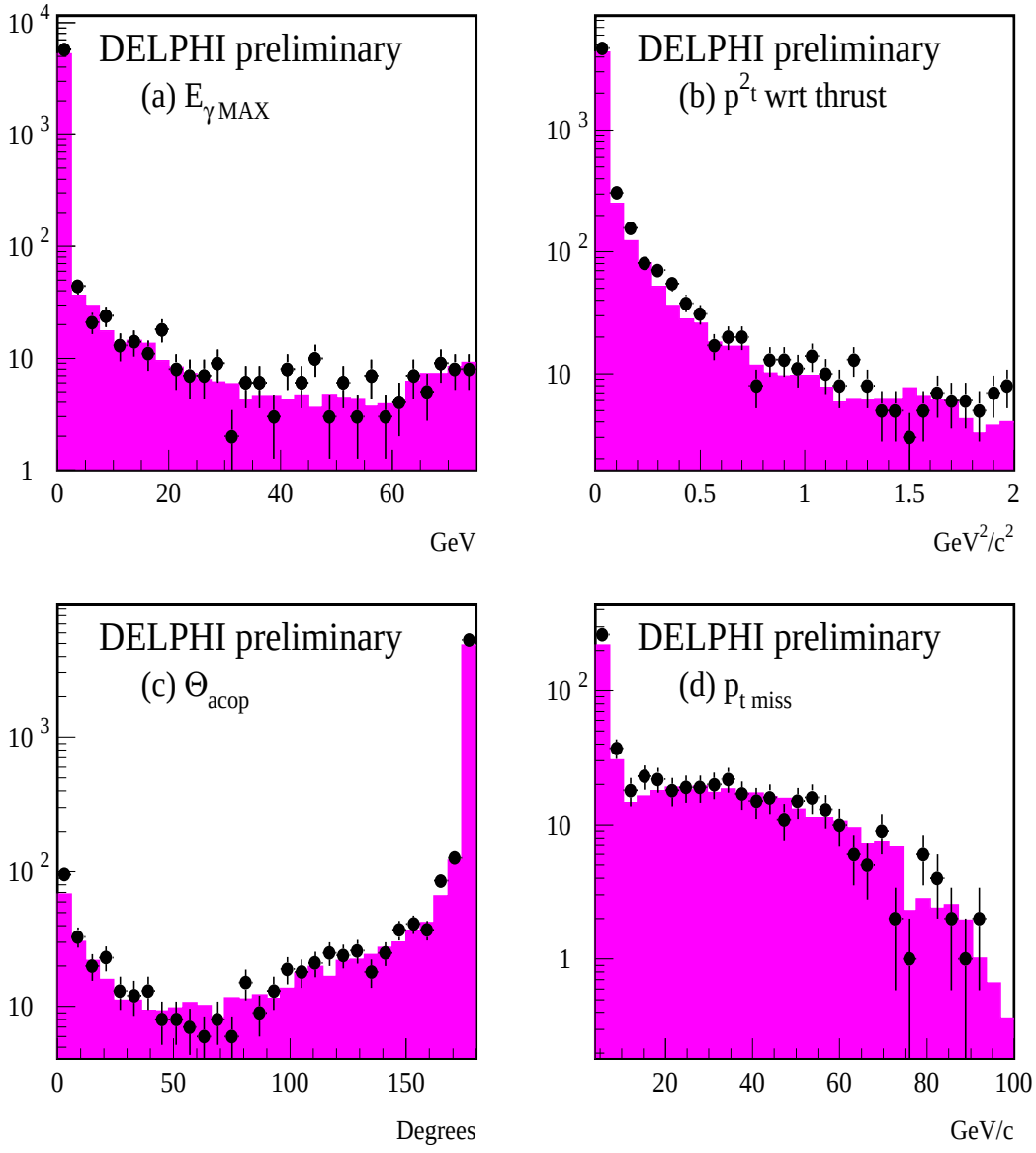

Figure 6: A pre-selection comparison of data and simulation in the stau analysis. The plots show: (a) Energy of the most energetic, isolated photon (b) The square of the transverse momentum with respect to the thrust axis (c) The acoplanarity. (d) Missing transverse momentum. The dots with error bars show the data, while the simulation is shown shaded.

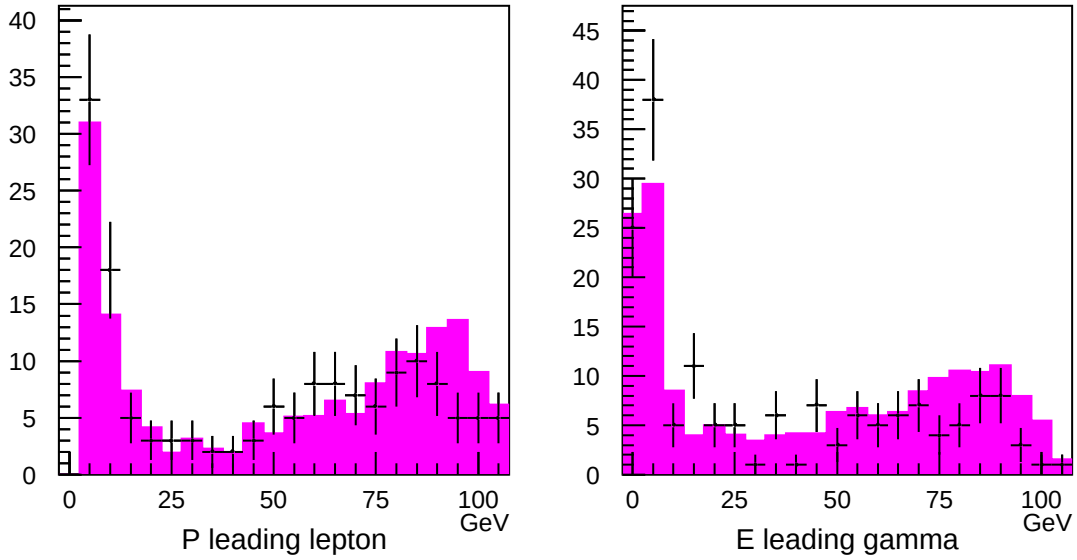

Figure 7: Comparison between the real data and the MC for the momentum of the leading lepton (left) and leading γ (right) in the standard $ee\gamma\gamma$ sample.

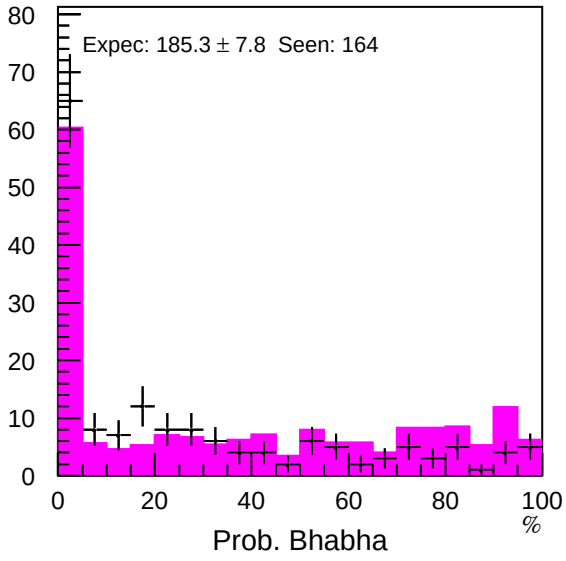

Figure 8: Bhabha tagging probability from the likelihood. The flat distribution ranging from 0 to 100% corresponds to the Bhabha events, while the events entering in the first bin are those from the other channels, like $\gamma\gamma$ events.

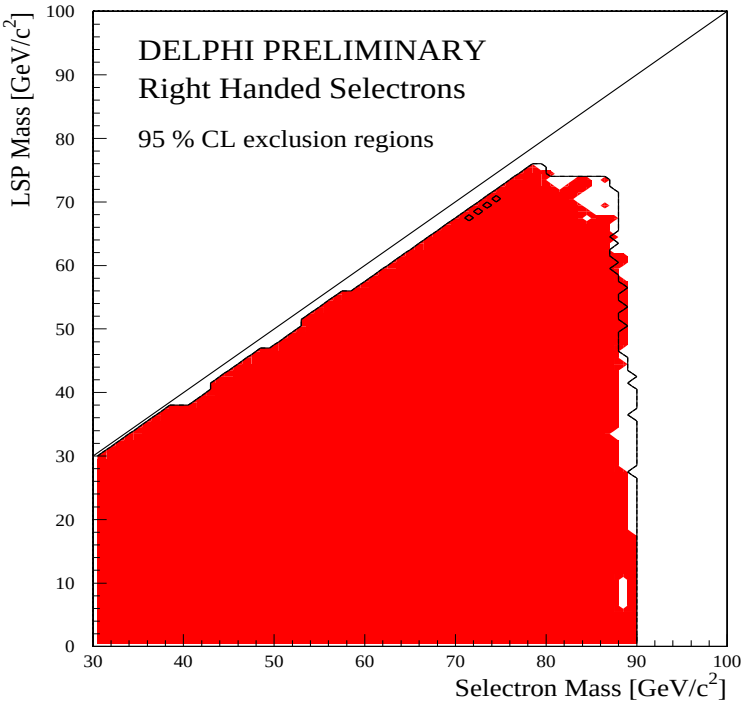

Figure 9: 95% CL exclusion region for $\tilde{e}_R$ in the $(M_{\tilde{e}}, M_{\tilde{\chi}^0_1})$ plane using data taken at centre-of-mass energies of $\sqrt{s}$ = 183 to 189 GeV. The shaded region shows the obtained exclusion limit, and the solid line shows the expected limit treating simulated background as data. For the exclusion limits value of tan(β)=1.5 and μ = -200 are used.

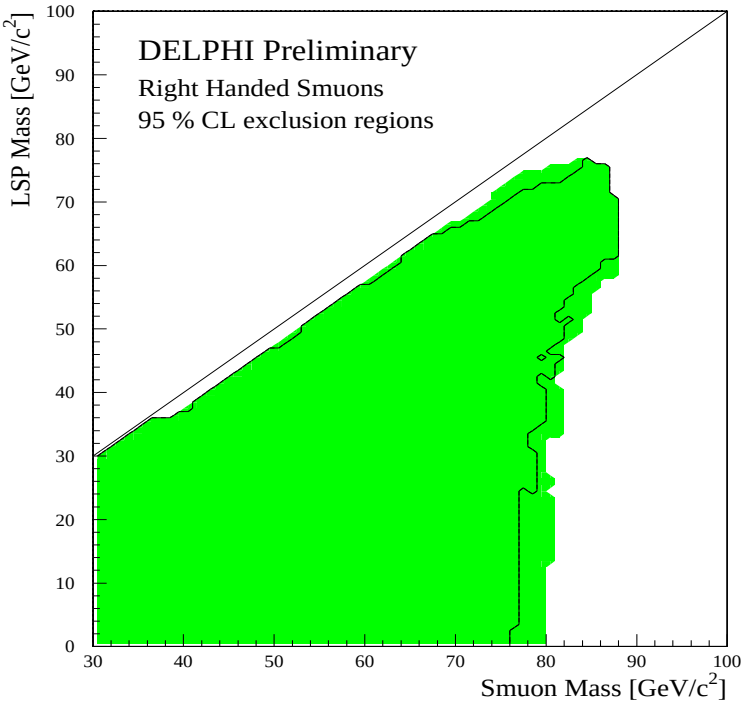

Figure 10: 95% CL exclusion region for $\tilde{\mu}_R$ in the ($M_{\tilde{\mu}}$,$M_{\tilde{\chi}^0_1}$) plane using data taken at centre-of-mass energies of $\sqrt{s}$ = 183 to 189 GeV. The shaded region shows the obtained exclusion limit, and the solid line shows the expected limit treating simulated background as data. For the exclusion limits value of tan(β)=1.5 and μ = -200 are used.

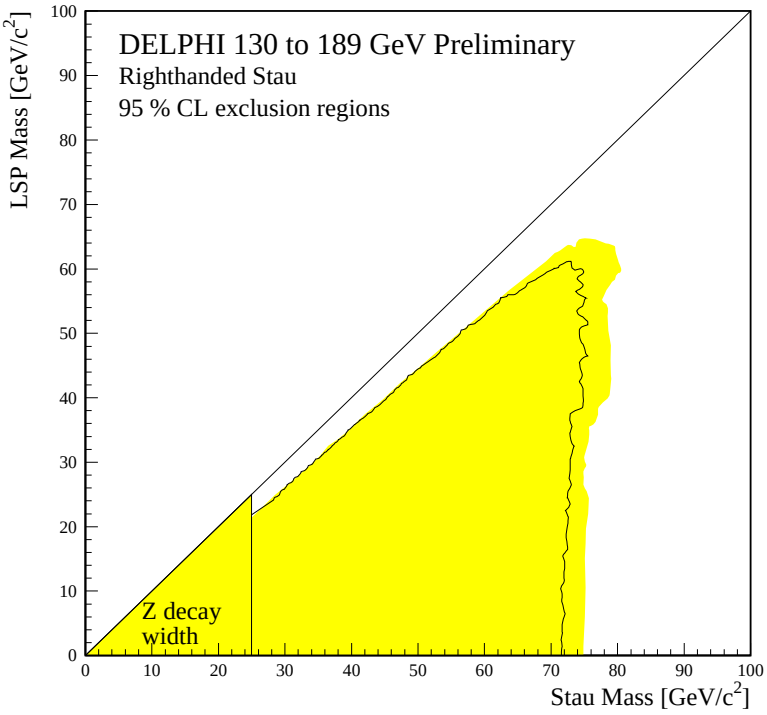

Figure 11: Mass limits for scalar stau 95% CL exclusion region for $\tilde{\tau}_R$ in the ($M_{\tilde{\tau}_R}$,$M_{\tilde{\chi}_1^0}$) plane. The shaded region shows the obtained exclusion limit, and the solid line shows the expected limit treating simulated background as data.

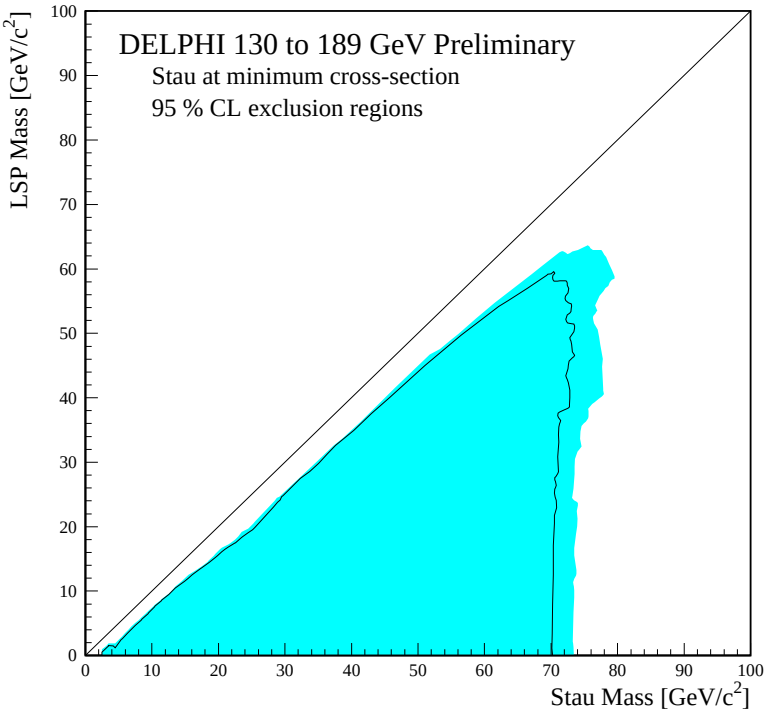

Figure 12: Mass limits for scalar stau 95% CL exclusion region for $\tilde{\tau}$ at minimal cross-section in the ($M_{\tilde{\tau}}$,$M_{\tilde{\chi}^0_1}$) plane. The shaded region shows the obtained exclusion limit, and the solid line shows the expected limit treating simulated background as data.

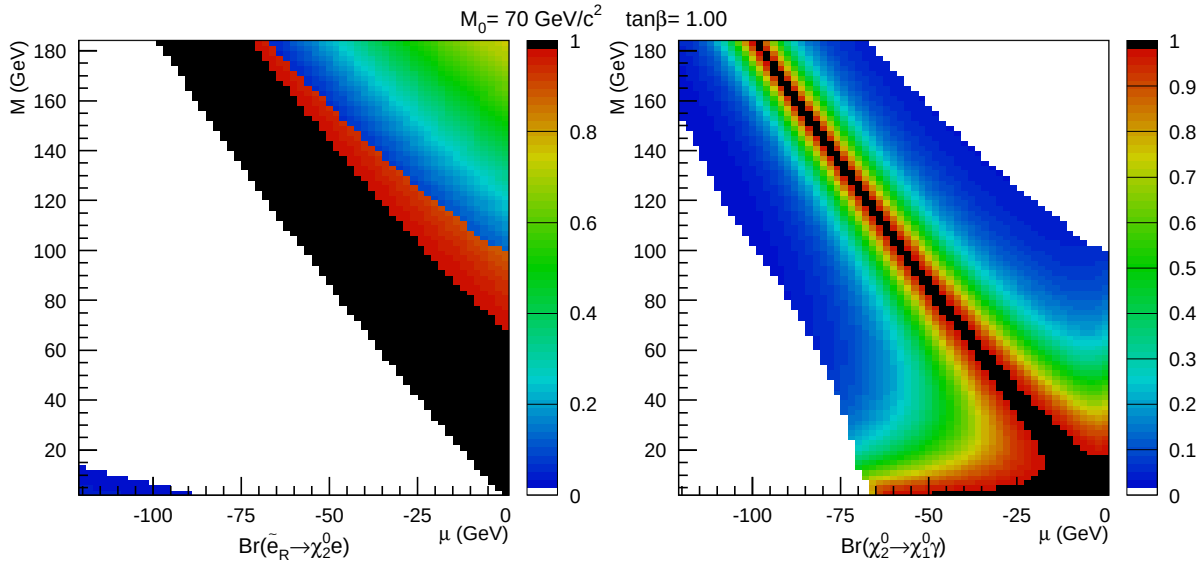

Figure 13: Branching ratios of the $\tilde{e} \to e\tilde{\chi}_2^0$ and $\tilde{\chi}_2^0 \to \tilde{\chi}_1^0\gamma$ for $M_0 = 70$ GeV/c^2 and $\tan\beta = 1$.

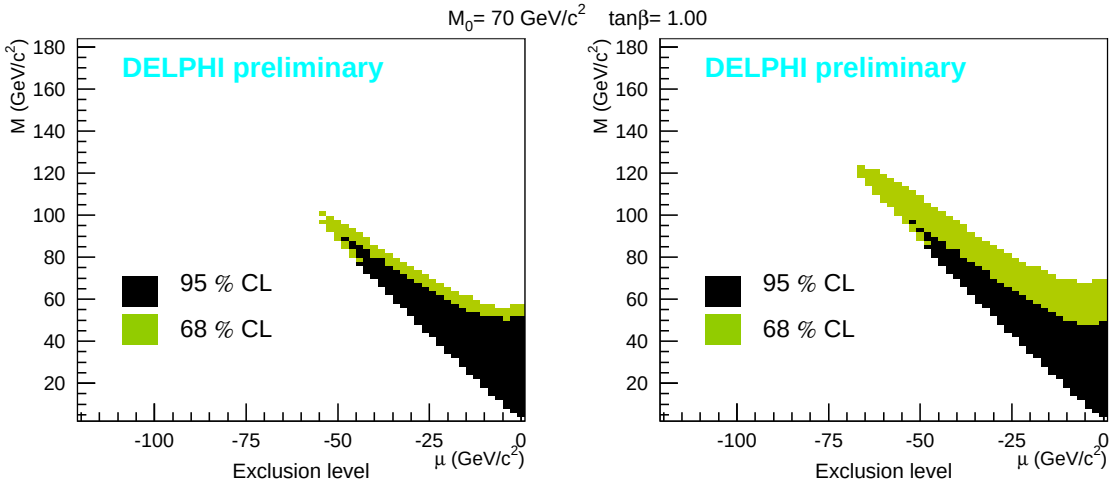

Figure 14: Exclusion regions at 95 and 68% C.L. in the SUSY parameter space from the $ee\gamma\gamma$ events (right) and $\mu\mu\gamma\gamma$ events (left).